

Supporting information for

Interfacial Cation Engineering in δ -MnO₂ Nanosheets for Efficient Oxygen Reduction Reaction

Dan Wu,^a Hao Wan,^b Zhicheng Zheng,^a Chengwei Kuang,^a Ning Zhang,^a Gen Chen,^{*a}
Xiaohe Liu^{*a,b} and Renzhi Ma^c

a. School of Materials Science and Engineering and State Key Laboratory of Powder Metallurgy, Central South University, Changsha 410083, China. E-mail: geenchen@csu.edu.cn

b. Zhongyuan Critical Metals Laboratory, Zhengzhou University, Zhengzhou 450001, China. E-mail: liuxh@csu.edu.cn

c. International Center for Materials Nanoarchitectonics (WPI-MANA), National Institute for Materials Science (NIMS), Namiki 1-1, Tsukuba, Ibaraki 305-0044, Japan

Experimental Section

Preparation of δ -MnO₂ monolayers. Typically, a 80 mL mixed solution containing 0.6 M Tetrabutylammonium Hydroxide (TBAOH) and 3 wt% H₂O₂ was prepared. Separately, a 40 mL aqueous solution of 0.3 M MnCl₂·4H₂O was formulated. The former solution was rapidly introduced into the manganese precursor solution with lots of bubbles generated. The obtained solution was aged overnight, followed by centrifugation at 10000 rpm for 20 min to obtain the supernatant containing δ -MnO₂ monolayers.

Flocculation. The colloidal suspension containing δ -MnO₂ monolayers was exposed to various salt solution (1 M LiCl, CsCl, DADMAC and PDDA solution) dropwise. The flocculation product was water-washed, freeze-dried and then collected. The composite containing different interlayer anions was denoted as MnO₂-M, where M stands for either lithium ion (Li⁺), cesium ion (Cs⁺), ammonium ion (DADMA⁺) or poly dimethyl diallyl ammonium ion (PDDA⁺).

Structural and morphological Characterization. X-ray diffraction (XRD) pattern was recorded with Rigaku D/max 2500VB+ (Cu K α radiation, λ = 1.5418 Å). Scanning electron microscope (Sirion 200) and transmission electron microscope (Tecnai G2 F20) were used to study the microstructural details of the products. The height of monolayer nanosheets was acquired on an atomic force microscope (AFM, Hitachi AFM5100N). XPS characterization was conducted with Thermo ESCALAB 250XI.

Electrochemical measurements. All the electrochemical measurements were performed on CH Instruments model 760E electrochemical workstation coupled with a three-electrode configuration at ambient temperature. Graphite rod, Hg/HgO electrode and 0.1 M KOH solution acted as counter electrode, reference electrode and electrolyte, respectively. To fabricate catalyst ink, 5 mg flocculated product and 2.5 mg super P were mixed together and then dispersed into a mixed water-isopropanol solution (1000 μ L, v/v = 3:1), and 10 μ L Nafion (10 wt%) was added subsequently. The working electrode was prepared by dripping catalyst ink onto a polished carbon glassy electrode (diameter = 3 mm) to enable the mass loading as 0.21 mg cm⁻². All the potentials were calibrated to the reversible hydrogen electrode (RHE) scale according to the equation: $E_{(vs\ RHE)} = E_{(vs\ Hg/HgO)} + E_{(Hg/HgO)} + 0.059 \times pH$. The polarization curves were recorded in O₂- and N₂-saturated electrolytes at the scan rate of 10 mV s⁻¹ with 95% iR compensation, separately.

Electrochemical impedance spectra (EIS) were tested at the potential of 0.615 V vs RHE in the frequency range of 10000 ~ 0.1 Hz with an alternating current voltage amplitude of 5 mV. Cyclic voltammetry (CV) curves at the incremental rate of 20, 40, 60, 80, 100 mV s⁻¹ were used to estimate the electrochemical surface area (ECSA).

DFT calculation. Density functional theory (DFT) calculations were carried out using the Vienna Ab Initio Simulation Package (VASP) in combination with the projector augmented wave (PAW) method.^{1,2} The exchange-correlation effects were described by the generalized gradient approximation (GGA) with the Perdew-Burke-Ernzerhof (PBE) functional.³ To minimize artificial interactions between periodic images, a vacuum layer of 20 Å was applied perpendicular to the plane, along with a 5 Å buffer at the bottom. A plane-wave cut-off energy of 400 eV was used, and electronic self-consistency was achieved with an energy convergence criterion of 10⁻⁵ eV. For structural optimization, a Γ -centered 3×4×1 k-point mesh was employed.

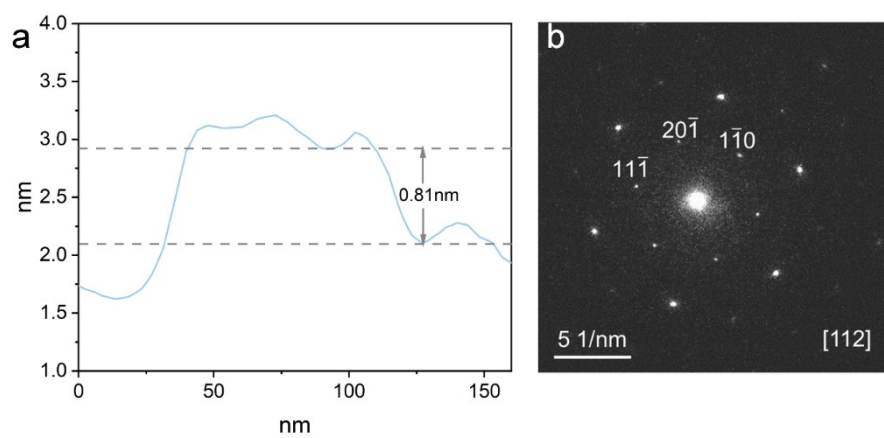


Fig. S1 (a) AFM heigh, (b) SAED pattern of MnO₂ monolayer.

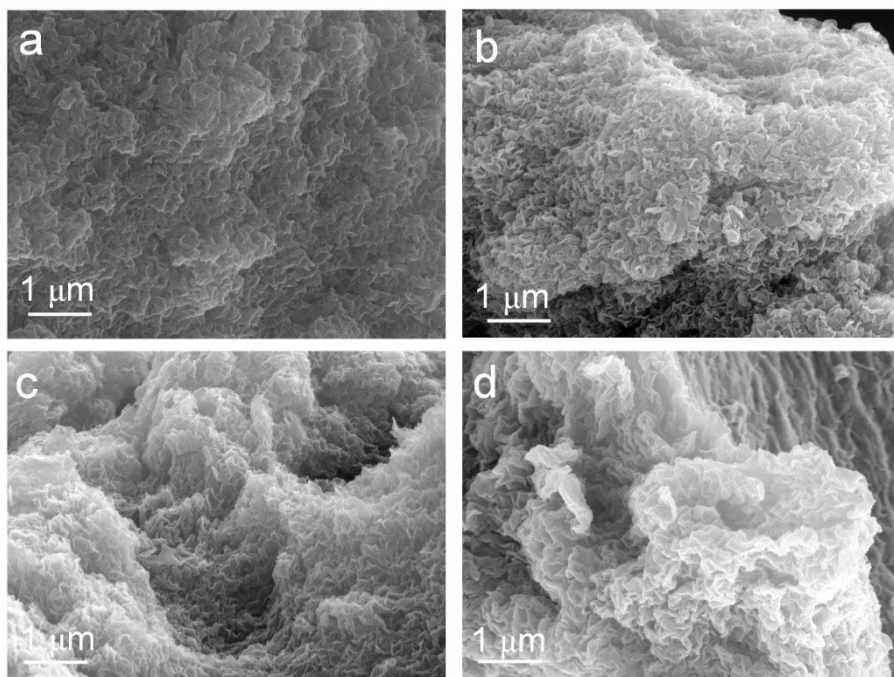


Fig. S2 SEM images of (a) MnO₂-Li, (b) MnO₂-Cs, (c) MnO₂-DADMA, (d) MnO₂-PDDA.

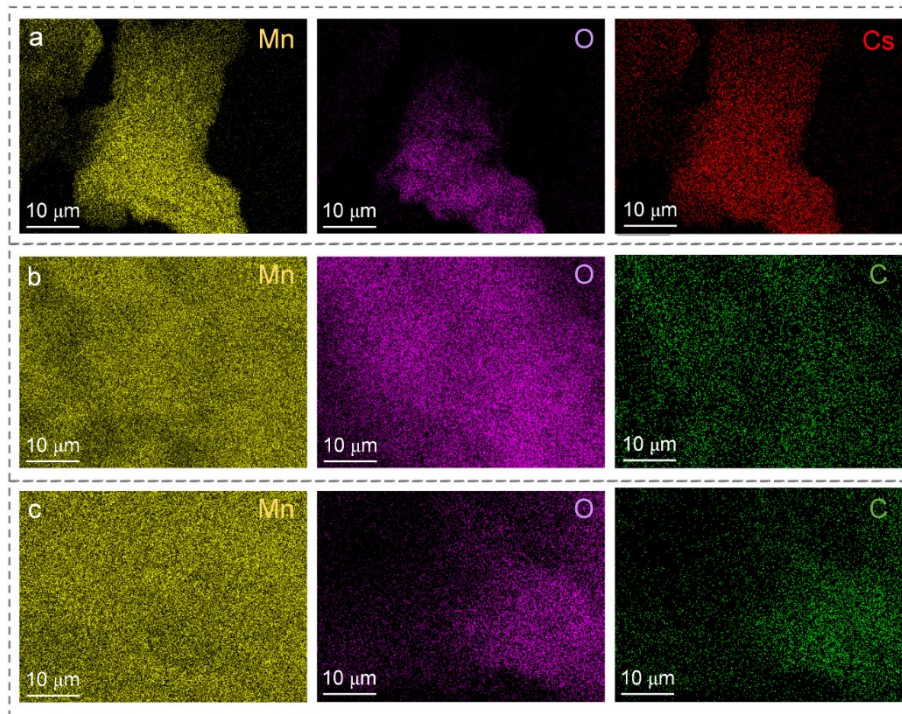


Fig. S3 EDS mapping images of (a) MnO₂-Cs, (b) MnO₂-DADMA, (c) MnO₂-PDDA.

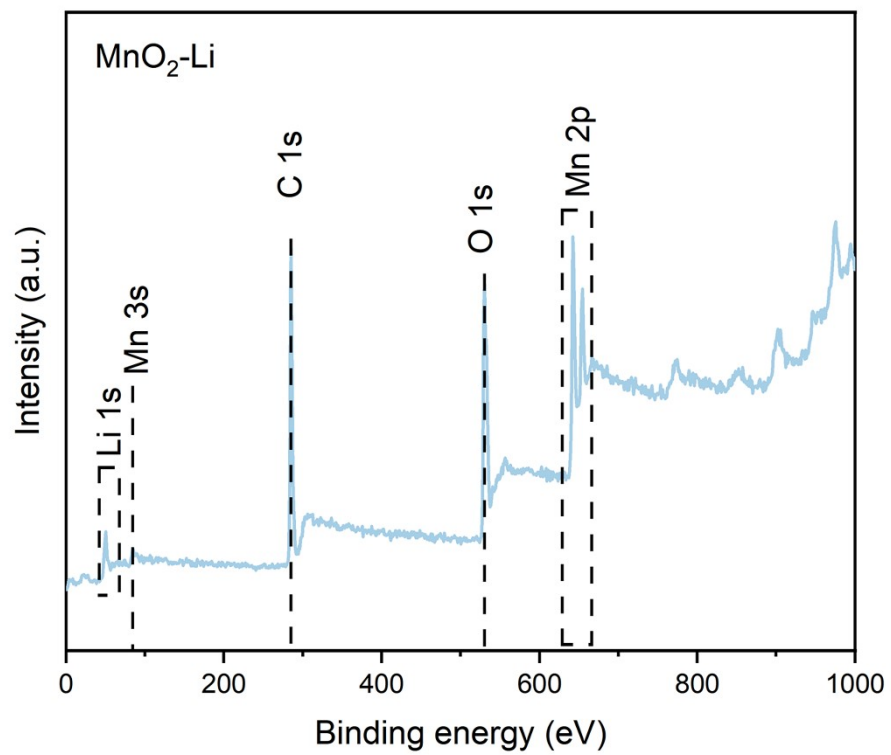


Fig. S4 XPS spectrum of MnO₂-Li.

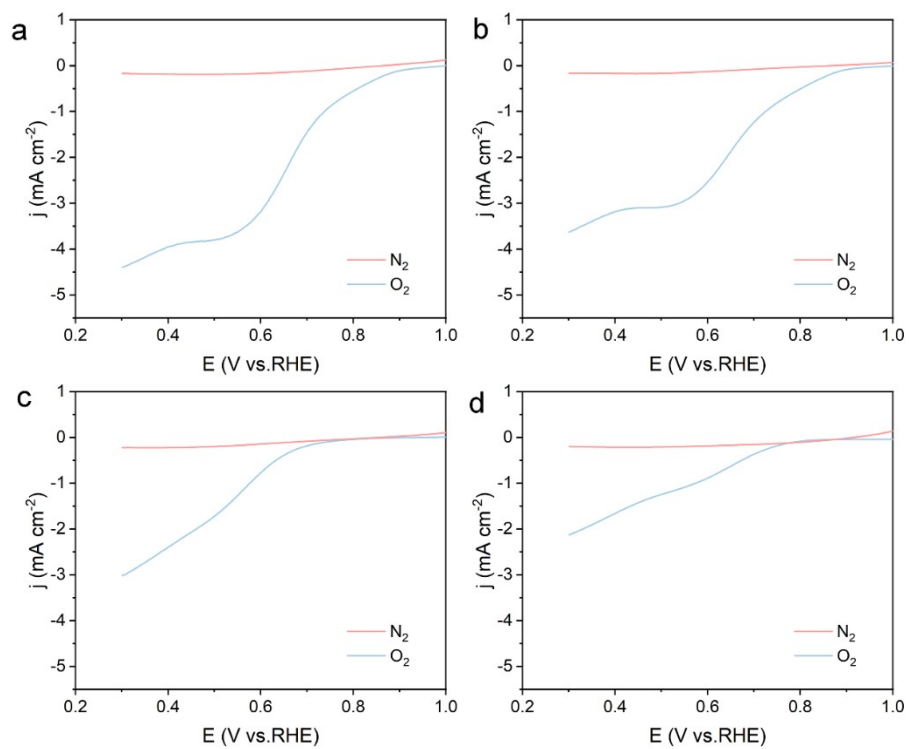


Fig. S5 Polarization curves in N_2 - or O_2 -saturated 0.1 M KOH solution of (a) MnO_2 -Li, (b) MnO_2 -Cs, (c) MnO_2 -DADMA, (d) MnO_2 -PDDA at 1600 rpm.

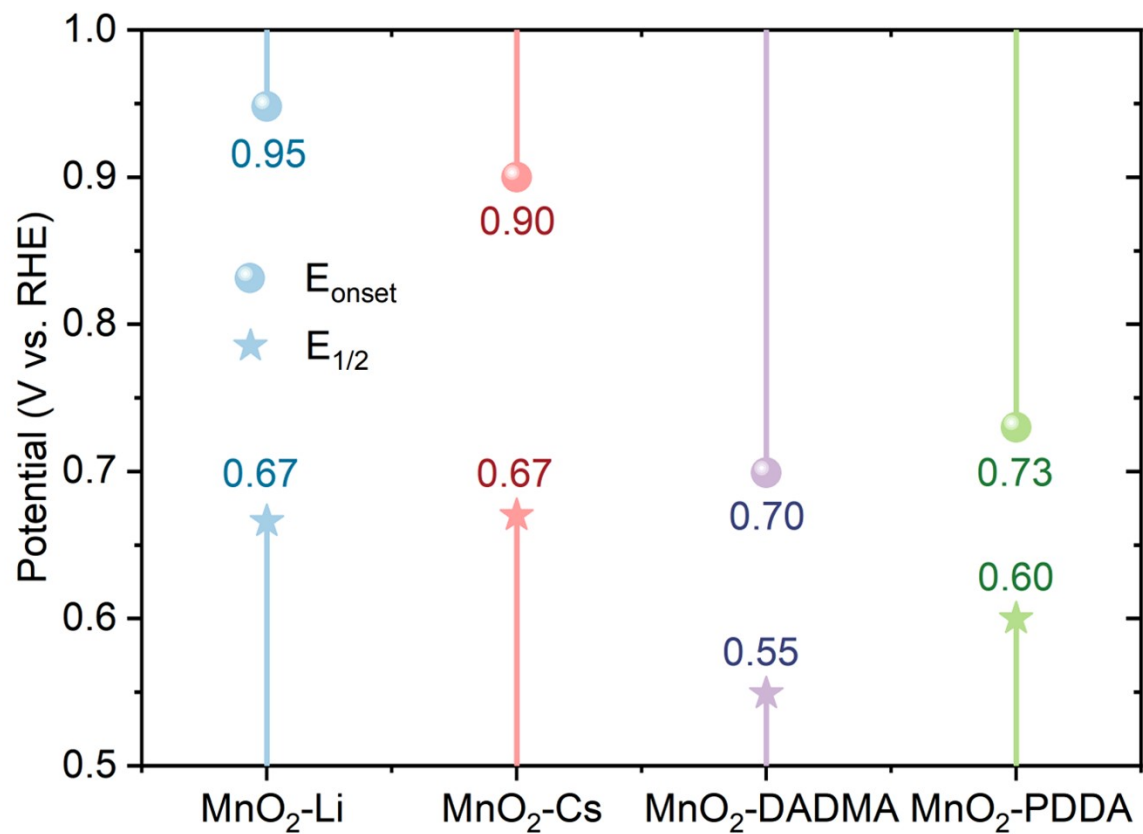


Fig. S6 E_{onset} and $E_{1/2}$ of MnO₂-Li, MnO₂-Cs, MnO₂-DADMA and MnO₂-PDDA.

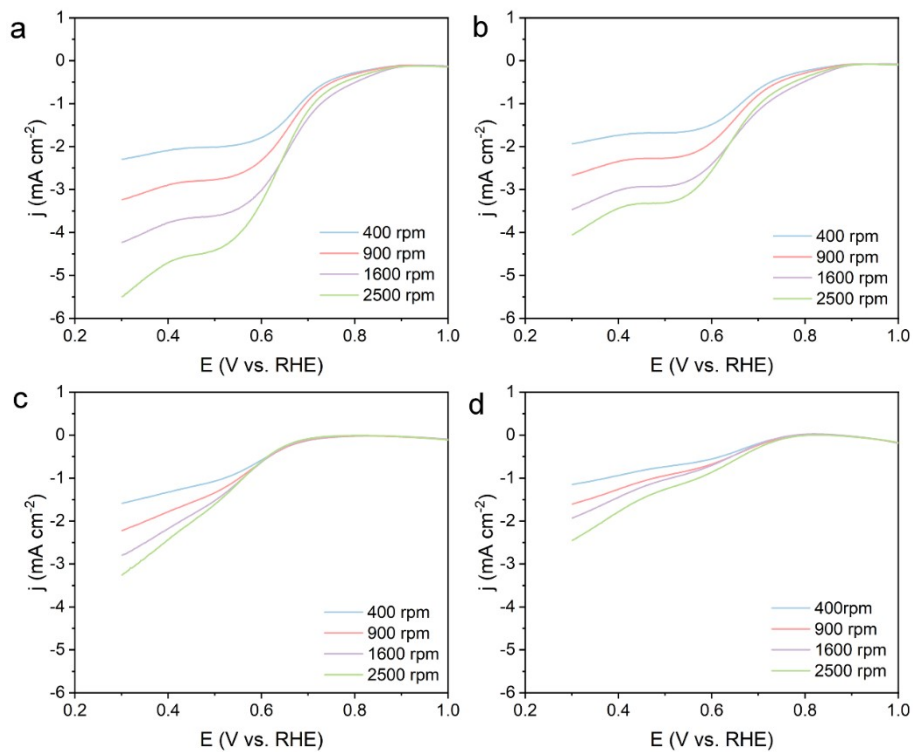


Fig. S7 Polarization curves of (a) MnO₂-Li, (b) MnO₂-Cs, (c) MnO₂-DADMA, (d) MnO₂-PDDA at different rotating rates.

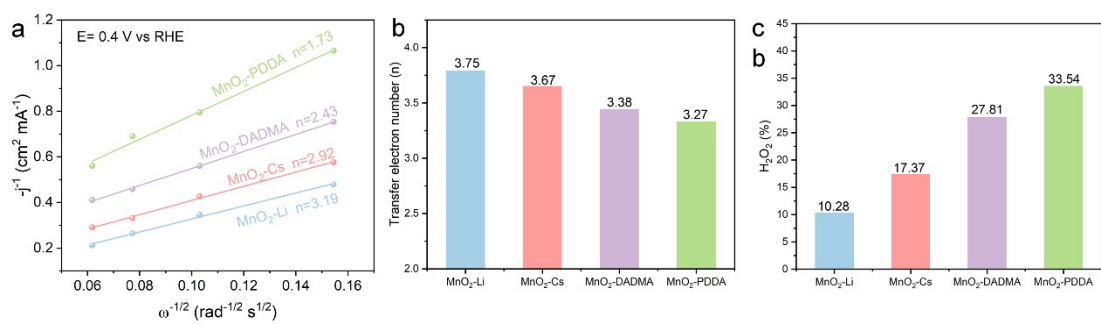


Fig. S8 Calculated electron transfer number obtained with (a) K-L methods (b) RRDE methods at the potential of 0.4 V vs. RHE. (c) the yield of H₂O₂ at the potential of 0.4V vs. RHE.

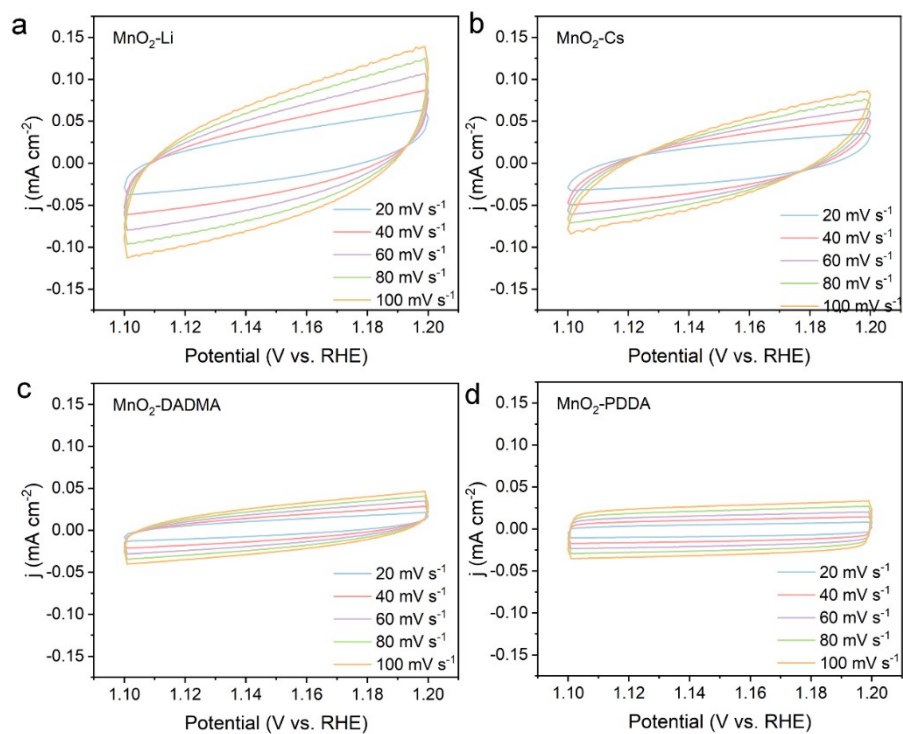


Fig. S9 CV curves of (a) MnO₂-Li, (b) MnO₂-Cs, (c) MnO₂-DADMA, (d) MnO₂-PDDA at different scan rate.

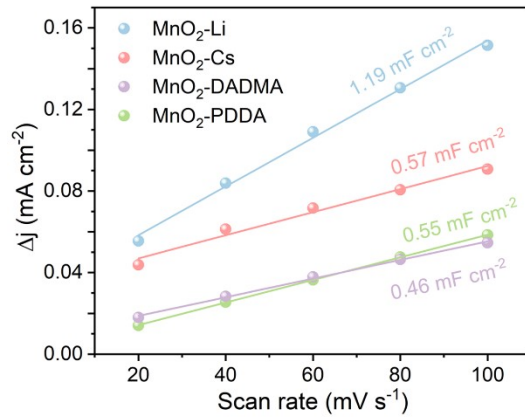


Fig. S10 current density as a function of scan rate of MnO_2 -M (M=Li, Cs, DADMAC, PDDA) nanosheets.

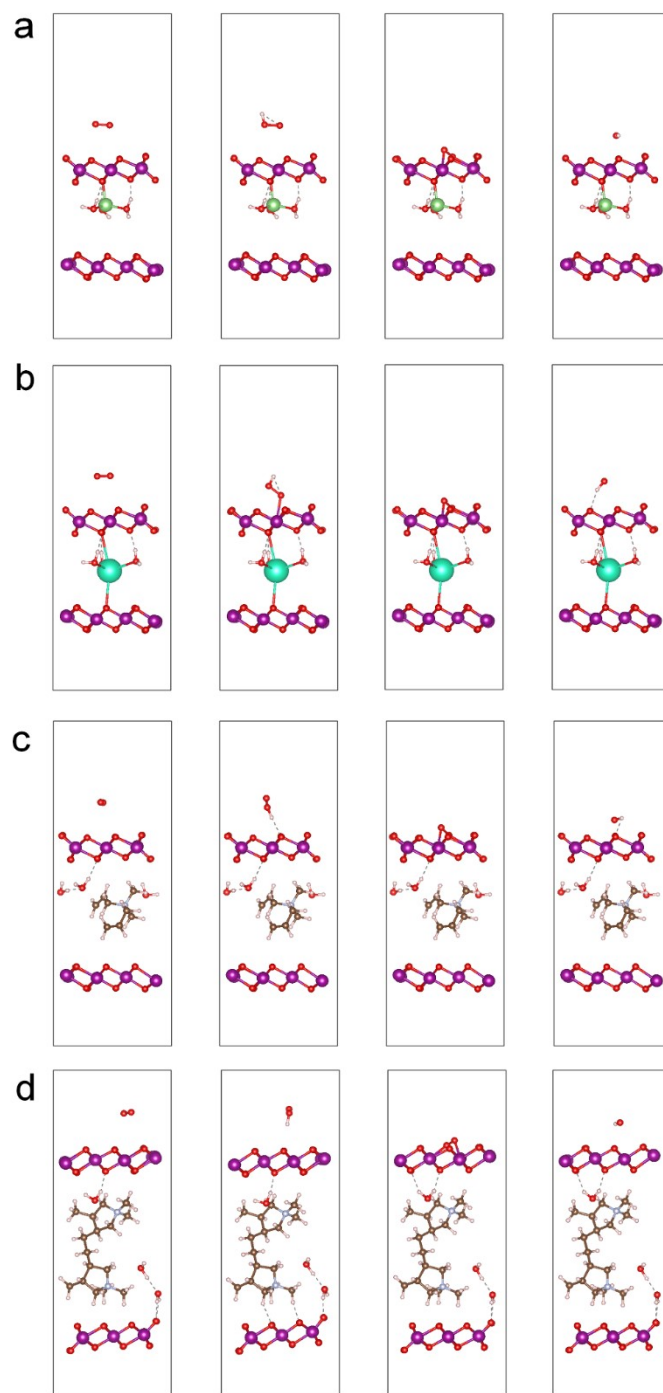


Fig. S11 Optimized configuration of adsorbed intermediate on (a) MnO₂-Li, (b) MnO₂-Cs, (c) MnO₂-DADMA, (d) MnO₂-PDDA.

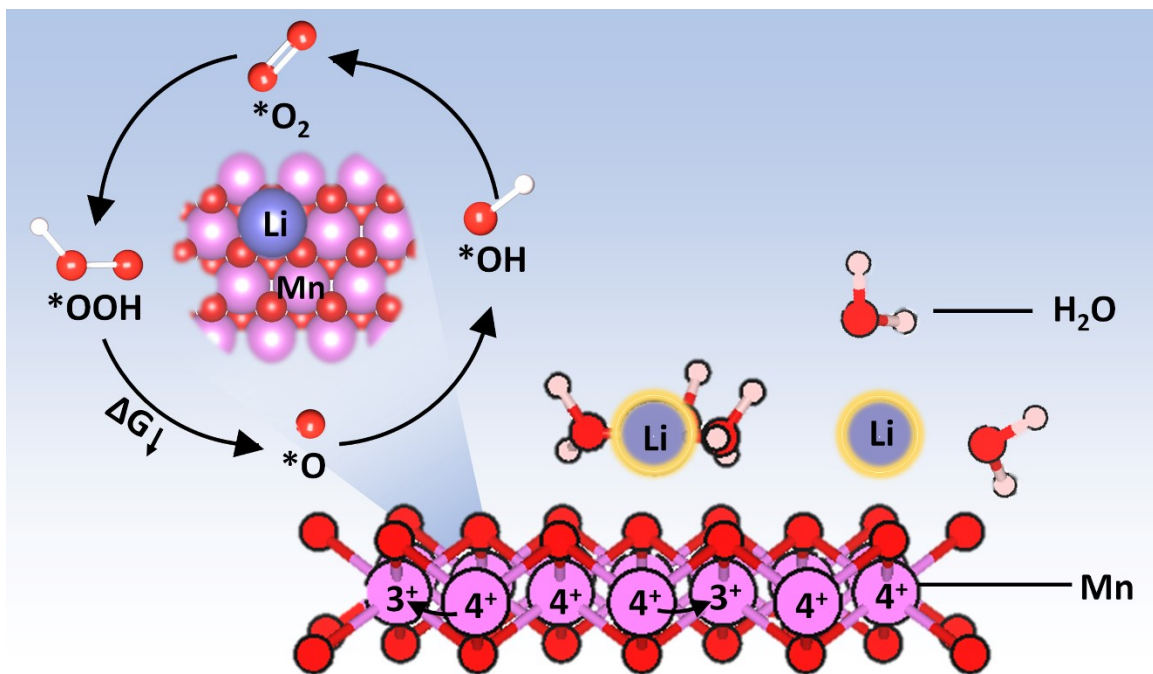


Fig. S12 schematic illustration of the enhanced ORR mechanism on MnO₂-Li.

Table S1. The fitting parameters of the simulated equivalent circuit in the inset of Fig. 5c.

	MnO₂-Li	MnO₂-Cs	MnO₂- DADMA	MnO₂-PDDA
R_s	70.83	82.4	84.1	78
R_{ct}	1173	4610	7450	41133

Reference

1. G. Kresse and J. Furthmüller, *Phys. Rev. B*, 1996, **54**, 11169–11186.
2. G. Kresse and D. Joubert, *Phys. Rev. B*, 1999, **59**, 1758–1775.
3. J. P. Perdew, K. Burke and M. Ernzerhof, *Phys Rev Lett*, 1996, **77**, 3865–3868.